# Inhibition of Nonpremixed Hydrogen Flames by $CF_3Br$

Leonard Truett, Hans Thermann, Dietmar Trees, and Kal Seshadri
Center for Energy and Combustion Research
Department of Applied Mechanics and Engineering Sciences
University of California at San Diego
La Jolla, California 92093-0411

and

Jessie Yuan, Leah Wells, and Paul Marshall
Department of Chemistry
University of North Texas
P. O. Box 305070
Denton, Texas 76203-5070

Corresponding author:
K. Seshadri
Center for Energy and Combustion Research
Department of Applied Mechanics and Engineering Sciences
University of California at San Diego
La Jolla, California 92093-0411
Phone: (619) 534-4876. Fax: (619) 534-5354.
email: seshadri@ames.ucsd.edu

**Abbreviated Title: Inhibition of Hydrogen Flames by $CF_3Br$**

Twenty-Seventh International Symposium on Combustion
University of Colorado at Boulder
August 2—7, 1998.

# Inhibition of Nonpremixed Hydrogen Flames by $CF_3Br$

Leonard Truett, Hans Thermann, Dietmar Trees, and Kal Seshadri
Center for Energy and Combustion Research
Department of Applied Mechanics and Engineering Sciences
University of California at San Diego
La Jolla, California 92093-0411

and

Jessie Yuan, Leah Wells and Paul Marshall
Department of Chemistry
University of North Texas
P. O. Box 305070
Denton, Texas 76203-5070

**Abstract**

Experimental and numerical studies are performed to elucidate the fundamental chemical mechanisms by which $CF_3Br$ inhibits nonpremixed hydrogen flames. These studies are motivated by previous work, which shows that $CF_3Br$ and its decomposition products inhibit hydrocarbon flames primarily by reacting directly with the radicals and by depleting radicals in the region where hydrogen and carbon monoxide are oxidized to form water and carbon dioxide. The elementary reaction $CF_3Br + H = CF_3 + HBr$ plays a prominent role in flame inhibition, but there are considerable uncertainties in the value of the rate parameters for this reaction. In view of these uncertainties, the rate of this reaction is measured directly by employing the flash-photolysis resonance fluorescence (FP-RF) technique and is compared with that predicted using transition state theory based on *ab initio* calculations. Predicted and measured rate parameters agree well, but differ significantly from those used in previous studies. The improved rate parameters are tested by conducting numerical computations and experiments on flames stabilized between two counterflowing streams. The fuel stream is a mixture of hydrogen and nitrogen and the oxidizing stream consists of air and $CF_3Br$. The strain rate at extinction is measured and given as a function of the concentration of $CF_3Br$ in the oxidizing stream. Numerical calculations are performed at conditions identical to those used in the experiments using detailed chemistry. Two different chemical-kinetic mechanisms are used. The chemical-kinetic mechanism describing the oxidation of the fuel is the same in both mechanisms, but the inhibition chemistries are different. One of the mechanisms has not been tested before on nonpremixed flames. One mechanism is found to generally overpredict and the other to underpredict the inhibiting effect of $CF_3Br$. The degree of overprediction and underprediction is evaluated using asymptotic theory. The differences between the mechanisms are discussed.

## Introduction

A number of experimental and numerical studies have been published on the influence of $CF_3Br$ on the structure and mechanisms of extinction of nonpremixed flames [1–10]. The chemical-kinetic mechanism developed by Westbrook [11] was employed in some of these previous studies to calculate the critical conditions of extinction of nonpremixed methane flames and the results were compared with measurements [4, 8–10]. In general, the inhibiting effect of $CF_3Br$ predicted by the chemical-kinetic mechanism was found to be stronger than that measured. Here an experimental and numerical study is conducted to elucidate the inhibiting effect of $CF_3Br$ on counterflow nonpremixed hydrogen flames. Critical conditions of extinction are measured. Numerical calculations are performed using detailed chemistry to determine the critical conditions of extinction. The numerical results are compared with measurements.

In nonpremixed flames burning heptane and methane, which are inhibited by $CF_3Br$, chemical reactions are found to take place in three layers—the fuel-consumption layer, the oxidation layer, and the $CF_3Br$-consumption layer [5–10]. In the fuel-consumption layer, the fuel reacts with radicals and the intermediate compounds CO and $H_2$ are formed. Carbon monoxide and hydrogen are oxidized in the oxidation layer. In the $CF_3Br$-consumption layer, the inhibitor is consumed. The principal mechanism by which $CF_3Br$ was found to inhibit the flame was by removing radicals in the oxidation layer as well as in the $CF_3Br$-consumption layer [5–10]. Since hydrocarbon chemistry is negligibly small in these layers, for simplicity the present study is conducted on hydrogen flames. The set of elementary reactions describing the oxidation of $H_2$ is a subset of detailed chemical-kinetic mechanisms describing the oxidation of most hydrocarbon fuels. Therefore, studies on inhibition of $H_2$ flames are useful for elucidating the mechanisms of inhibition of hydrocarbon flames.

Previous studies [9, 10] have shown that in the $CF_3Br$-consumption layer, the key reactions responsible for consuming the inhibitor are the steps $CF_3Br + H \rightarrow CF_3 + HBr$ and the unimolecular thermal decomposition reaction $CF_3Br \rightarrow CF_3 + Br$. There are considerable uncertainties on the values of the rate parameters for these elementary reactions. Figure 1 shows the rate constant of the reaction $CF_3Br + H \rightarrow CF_3 + HBr$ in the Arrhenius form measured by a number of investigators. The rate parameters obtained at temperatures less than 400 K by isolated reaction techniques [12–14] are different from those obtained at temperatures greater than 700 K by fitting the kinetics of multireaction systems [15–19]. This fitting is uncertain, as evidenced by the larger than an order of magnitude spread among the values of the rate constant of this reaction at 1000 K. In view of these uncertainties, the rate of this reaction is measured employing the flash-photolysis resonance fluorescence (FP-RF) technique. The measurements bridge the gap between the previous low and high temperature regimes and provide a new rate expression which is used in the numerical model. The mea-

sured rate is compared with that calculated using transition state theory based on *ab initio* calculations. As will be seen, the rate expression used previously for $CF_3Br + H \rightarrow CF_3 + HBr$ underestimates the contribution of this reaction to the consumption of $CF_3Br$.

## Experimental Apparatus and Procedure

### Extinction Experiments

The counterflow burner used to obtain the critical conditions of extinction is described in detail elsewhere [8, 9]. The burner is made up of two opposing ducts with inner diameter of 22.2 mm through which gaseous reactants are introduced. The distance between the ducts is 10 mm. A steady flame can be stabilized in the region between the opposing ducts for long periods of time. The fuel stream, a mixture of $H_2$ and $N_2$, is introduced from one duct. The oxidizing stream consisting of air and $CF_3Br$ is introduced from the other duct. The flowrates of $H_2$, $N_2$, air, and $CF_3Br$ are measured using computer-regulated electronic mass flow controllers. The calibrated accuracy of these mass flow controllers is $\pm 1\%$. The velocities of the reactants at the exits of the ducts are presumed to be equal to the ratio of the volumetric flowrates to the exit areas. For the range of flow velocities encountered in the experiments (up to 1.87 m/s), the flow is laminar since the Reynolds numbers based on the exit diameters of the ducts are less than 2500. Seshadri and Williams [20] have shown that for laminar flow in the counterflowing configuration employed here, if the Reynolds number is large enough and if the values of the tangential component of the flow velocities at the exits of ducts are zero, then the flow-field comprises two inviscid rotational regions on either side of a thin viscous region formed in the vicinity of the stagnation plane. The strain rate $a$, defined as the normal gradient of the normal component of the flow velocity in the inviscid region on the oxidizer side of the stagnation plane, is given by the expression [20]

$$a = \frac{2|V_2|}{L}\left(1 + \frac{|V_1|\sqrt{\rho_1}}{|V_2|\sqrt{\rho_2}}\right), \tag{1}$$

where subscripts 1 and 2, respectively, denote conditions in the fuel stream and in the oxidizing stream at the exit plane of the ducts, $V$ is the velocity, and $\rho$ the density. The strain rate calculated from Eq. (1) is taken as a measure of the characteristic flow time of the reactants in the flame. At extinction it is denoted by $a_q$.

All measurements are made at atmospheric pressure and the temperatures of the reactants at the exit of the ducts $T_1 = T_2 = 298\,\mathrm{K}$. To ensure that the flame position, which is typically close to that of the stagnation plane, is approximately in the middle of the two ducts, experiments are performed such that the momentums of the counterflowing streams at the exit of the ducts, represented by the product of the density and the square of the flow

velocity, are nearly the same. Experiments are performed for mixtures with 16% $H_2$ and 84% $N_2$ and with 15% $H_2$ and 85% $N_2$ by volume in the fuel stream. First the flame is stabilized in the burner for a chosen amount of $CF_3Br$ in the oxidizing stream. Then the velocities are gradually increased until the flame extinguishes. The strain rate at extinction is calculated using Eq. (1). The experiments are repeated for different amounts of $CF_3Br$ in the oxidizing stream.

## Flash-Photolysis Resonance Fluorescence (FP-RF) Technique for Measuring the Rate of $CF_3Br + H \rightarrow CF_3 + HBr$

The apparatus and its modifications for the study of reactions of atomic hydrogen are described elsewhere [21–23]. The H atoms are generated in the presence of a large excess of $CF_3Br$ by flash-lamp photolysis of a precursor. The precursors employed are $NH_3$ and $H_2O$. A gas-chromatographic analysis of the $CF_3Br$ revealed no impurities other than a trace of $N_2$, which is removed by freeze-pump-thaw cycles at 77 K. All reagents are diluted in a large excess of Ar bath gas which served to thermalize the photolytically produced H atoms, to raise the heat capacity of the reacting mixture, to maintain a constant temperature, and to slow diffusion of H atoms to the reactor walls (described by an effective first-order decay coefficient $k_{\text{diff}}$). Total pressures between 55 and 155 mbar are employed. The H-atom concentration is monitored by time-resolved resonance fluorescence at the Lyman-alpha wavelength, excited by a microwave-powered discharge through a flowing sample of $H_2$ diluted in Ar. The fluorescence signal, $I_f$, which is proportional to the molar concentration of H, represented by [H], is monitored with a solar-blind photomultiplier tube coupled to photon-counting electronics. The condition $[H] \ll [CF_3Br] \ll [Ar]$ ensured pseudo-first order kinetics $d[H]/dt = -k_{ps1}[H]$, where $k_{ps1} = k_m[CF_3Br] + k_{\text{diff}}$. Here $k_m$ is the measured rate constant of the reaction $CF_3Br + H \rightarrow CF_3 + HBr$, $[CF_3Br]$ and [Ar] are molar concentrations of $CF_3Br$ and Ar respectively, and $t$ is the time.

Figure 2 shows an exponential decay of [H] obtained from monitoring the fluorescence intensity, $I_f$, as a function of time, $t$, and a linear plot of observed $k_{ps1}$ values vs $[CF_3Br]$ with a slope equal to the bimolecular rate constant $k_m$. The residence time of the gas mixtures in the heated reactor was varied over 0.3–2.1 s to check for possible thermal decomposition, and the flash-lamp energy and concentration of precursor were varied over 2.5–6.1 J and $5\times10^{-10}$–$30\times10^{-10}$ mol/cm$^{-3}$ to verify that the measured $k_m$ was independent of the initial radical concentrations. This independence demonstrates that $k_m$ is isolated from secondary chemistry involving photolytic or reaction products.

Figure 1 summarizes the measurements, where $k_m$ determinations under a variety of conditions have been averaged at each temperature. The two H-atom precursors gave results

which fall on the same line. Above 900 K for $H_2O$ (750 K for $NH_3$) the observed $k_m$ increased sharply and unrealistically, which is attributed to pyrolysis reactions between $CF_3Br$ and the precursors, so these data were not considered further. An Arrhenius fit over 295–860 K yields $k_m = A_m \exp[-E_m/(RT)]$, where $T$ is the temperature, and $R$ the gas constant. The activation energy $E_m$ is 21.7±0.2 kJ/mol, and the frequency factor $A_m$ is $(4.2\pm0.2)\times10^{13}$ cm$^3$ mol$^{-1}$ s$^{-1}$. The uncertainties in the parameters are one standard deviation and represent precision only. Consideration of the covariance leads to 95% statistical confidence intervals for $k_m$ of about 3% in the center of the $T$ range increasing to 5% at the highest temperature and 10% at the lowest. Allowance of ± 5% for unrecognized systematic errors leads to accuracy limits of about 10% for $k_m$.

## Transition State Theory (TST) Analysis

Transition state theory (TST) is employed to calculate the rate of the reaction $CF_3Br + H \rightarrow CF_3 + HBr$. The reactants and transition state (TS) for this reaction have been characterized using Gaussian-2 theory. The methodology is detailed elsewhere [24, 25]. A brief description is given here. Molecular geometries and frequencies were obtained at HF/6-31G(d) and MP2=full/6-31G(d) levels of theory, then energies at the latter geometries were refined in a series of steps to approximate a QCISD(T)/6- 311+G(3df,2p) calculation. Results for $CF_3Br$ have already been shown to be in good accord with experiment [26]. The MP2=full/6-31G(d) geometry of the $C_{3V}$ symmetry TS has a linear H-Br-C group and F-C-Br angles of 109.0 degrees. The H-Br distance is 1.716, the C-Br distance is 2.088 and the C-F distance is 1.328, all in $10^{-10}$ m. The MP2=full/6-31G(d) vibrational frequencies, scaled by a standard factor of 0.95, are 1130i, 195 (2), 240 (2), 372, 502 (2), 754, 1052 and 1234 (2) cm$^{-1}$. The geometry and frequency information was employed in canonical transition state theory (TST) [27]: $k_c(T) = \Gamma(k_B T/h)[Q_{TS}/(Q_H Q_{CF_3Br})]\exp[-E_0^\ddagger/(RT)]$. Here $k_c$ is the rate constant of the reaction $CF_3Br + H \rightarrow CH_3 + HBr$, calculated using TST, $k_B$ is the Boltzmann constant, and $h$ the Planck's constant. The quantity $\Gamma$ is a quantum-mechanical tunneling correction based on the Eckart formalism [28], which varied from 3.7 at 298 K to 1.03 at 2000 K. Calculation of $\Gamma$ requires the forward barrier including zero-point energy at 0 K, $E_0^\ddagger$, the reverse barrier derived from $E_0^\ddagger$ and the reaction enthalpy at 0 K, −83.0 kJ mol$^{-1}$ [29], and the imaginary frequency given above. The $Q$'s are the partition functions of the TS (electronic degeneracy of 2 assumed) and reactants. The equation for $k_c$ was fitted to our measurements with $E_0^\ddagger$ as the single adjustable parameter, yielding $E_0^\ddagger = 21.8$ kJ mol$^{-1}$, in almost exact accord with the G2 value of 21.9 kJ mol$^{-1}$. This is an independent check of the accuracy of our measurements. This result is not very sensitive to the details of the tunneling model; if $\Gamma$ is fixed at unity (i.e. no tunneling) then the best fit value of $E_0^\ddagger$ is 19.1 kJ mol$^{-1}$. The TST rate constant, including Eckart tunneling, is given by $k_c(T) = 2.0\times10^7 T^{2.01}\exp(-1650/T)$ cm$^3$ mol$^{-1}$ s$^{-1}$. This is

compared with experiment in Fig. 1. The rate given by this equation extrapolates well to the values measured by Hidaka et al. [19]. Theirs was the simplest and most recent system to be modeled at high temperatures, shock-heated $CF_3Br/H_2$, and thus their values are probably the most reliable and are seen to be consistent with TST. Therefore we recommend the use of this rate over 295-2000 K. The widely used expression for the rate constant of $CF_3Br + H \rightarrow CF_3 + HBr$ from Baulch et al. [18] significantly underestimates its contribution to $CF_3Br$ destruction, especially at the lower end of their temperature range around 700 K.

## Formulation of the Numerical Problem

The conservation equations of mass, momentum and energy and the species balance equations used in the formulation of the numerical problem are summarized elsewhere [30–32]. The species balance equations include thermal diffusion and the energy conservation equation includes radiative heat losses from carbon dioxide and water vapor [32]. Calculations are performed in an axisymmetric configuration over a computational domain of 10 mm. The axial coordinate is $y$. The fuel boundary is presumed to be located at the plane $y = 0$, and the oxidizer boundary at the plane $y = 10\,\text{mm}$. At both ends of the computational domain the mass fractions of the various species in reactant mixtures and the normal components of the flow velocity are specified. The values of the tangential component of the flow velocity at both ends are set equal to zero. The characteristic strain rate at the stagnation plane is calculated using Eq. 1.

Two different chemical-kinetic mechanisms are used, referred to as Mechanism A and Mechanism B. Both mechanisms use elementary reactions 1–35, and 37–40b shown in Table 1 of Ref. [31], where reactions 1–17 describe the oxidation of hydrogen. Following previous studies, reactions involving compounds comprising two or more carbons are excluded [4, 9]. In both mechanisms, the improved rate constant for the reaction $CF_3Br + H = CF_3 + HBr$ is used ($2.0\times10^7 T^{2.01}\exp(-1650/T)\,\text{cm}^3\ \text{mole}^{-1}\ \text{s}^{-1}$). The two mechanisms differ in the description of the inhibition chemistry. Mechanism A uses the inhibition chemistry put together by Westbrook [11] and it is made up of reactions B1–B10, B15, B17, B18, B21–B38, B30–B36, B40–B46, and B48–B56 shown in Table II of Ref. [11]. Mechanism B uses the inhibition chemistry put together at the National Institute for Standards and Technology [33]. Mechanism B has been employed previously to evaluate the influence of halogenated compounds on the structure and burning velocities of premixed flames [34, 35]. The present work is the first test of predictions of Mechanism B of the critical conditions of extinction of nonpremixed flames.

## Results and Discussion

In Figs. 3 and 4 the strain rate $a_q$ is plotted as a function of the mole fraction of the inhibitor, $X_{CF_3Br,2}$, in the oxidizing stream. The points represent measurements and the lines are results of numerical calculation. In these figures, the region below any curve represents flammable mixtures. For $X_{CF_3Br,2} = 0$ and 16% $H_2$ by volume in the fuel stream, the measured $a_q = 680\,s^{-1}$ and the calculated $a_q = 587\,s^{-1}$. For $X_{CF_3Br,2} = 0$ and 15% $H_2$ by volume in the fuel stream, the measured $a_q = 450\,s^{-1}$ and the calculated $a_q = 412\,s^{-1}$. The differences between the calculated and measured $a_q$ are attributed to inaccuracies in the chemical-kinetic mechanism describing the oxidation of hydrogen and to uncertainties in the measurements. Figures 3 and 4 show $a_q$ to decrease with increasing $X_{CF_3Br,2}$. Calculations using Mechanism A overpredict this decrease, while calculations with Mechanism B underpredict this decrease. Thus, the two mechanisms bracket the inhibition efficiency of $CF_3Br$. In the following paragraphs, activation-energy asymptotic analysis is used to obtain quantitative measures of these rates.

In the asymptotic analysis of the flame structure, it is convenient to introduce a conserved scalar quantity $\xi$ called the mixture fraction, which satisfies a source-free conservation equation [36–39]. This conserved scalar is defined such that $\xi = 0$ at the oxidizer boundary and $\xi = 1$ at the fuel boundary [36–39]. A characteristic diffusion time $\chi^{-1}$ deduced from the spatial gradient $\xi$ can be written as:

$$\chi = 2[\lambda/(\rho c_p)]|\nabla\xi|^2, \tag{2}$$

where $\lambda$ is the thermal conductivity, $\rho$ the density, and $c_p$ the heat capacity per unit mass of the mixture. The quantity $\chi$ also represents the scalar dissipation rate and plays a central role in asymptotic analyses [37, 40, 41]. The strain rate $a$ influences the flame structure mainly through its influence on $\chi$. In asymptotic analyses of the structure of diffusion flames, it is convenient to use $\xi$ as the independent variable [37, 39–41]. The value of $\chi$ changes with $\xi$ [42]. Using asymptotic methods in which chemical reactions are presumed to take place in a thin reaction zone, Kim and Williams [43] have derived a formula relating $\chi$ to the strain rate $a$ which can be written as

$$\chi = \frac{a}{2\pi}\frac{3\left[(\rho_2/\rho_{st})^{0.5}+1\right]^2}{\left[2(\rho_2/\rho_{st})^{0.5}+1\right]}\exp\{-2[\mathrm{erfc}^{-1}(2\xi_{st})]^2\} \tag{3}$$

where $\xi_{st}$ is the stoichiometric mixture fraction and $\rho_{st}$ is the density evaluated at the adiabatic flame temperature $T_{st}$.

For simplicity, the chemical reaction between hydrogen and oxygen is represented by a one-step process $H_2 + (1/2)O_2 \rightarrow H_2O$. The rate constant for this overall reaction, $k_o$, is

written as $k_o = A_o \exp[-E_o/(RT)]$, where $A_o$ is the frequency factor and $E_o$ the activation energy. The reaction rate is presumed to be first-order with respect to the fuel and oxygen. The inhibitor $CF_3Br$ is presumed to be inert and preferential diffusion is neglected. These are poor assumptions for inhibited nonpremixed hydrogen flames; however, the rates of decrease of $a_q$ with increasing $X_{CF_3Br,2}$ are presumed not to be influenced greatly by these approximations. For one-step overall chemistry, the stoichiometric mixture fraction is given by $\xi_{st} = (1 + 8Y_{F,1}/Y_{O_2,2})^{-1}$ [36, 37], where $Y_{F,1}$ is the mass fraction of the fuel in the fuel stream, and $Y_{O_2,2}$ is the mass fraction of oxygen in the oxidizing stream. The adiabatic flame temperature is given by $W_F \int_{T_u}^{T_{st}} c_p dT = Y_{F,1}(-\Delta H)\xi_{st}$, where $(-\Delta H)$ is the heat release in the one-step reaction per mole of $H_2$ consumed, $W_F$ is the molecular weight of the fuel, and $T_u = T_1 = T_2 = 298$ K.

To check the accuracy with which $\chi_q$ can be calculated using Eqs. (1) and (3), the scalar dissipation rate at extinction is calculated numerically using Eq. (2). Detailed chemistry and detailed transport are used in this calculation. For uninhibited flames with 16 % $H_2$ by volume in the fuel stream, the scalar dissipation rate at extinction is $\chi_q = 225\,s^{-1}$. Using the injection velocities and concentrations of the reactants in the fuel and oxidizing streams at extinction, the strain rate is calculated using Eq. (1) and the scalar dissipation rate using Eq. (3). The value of $\chi_q$ is found to be $250\,s^{-1}$, which is very close to that obtained from the detailed numerical calculations. Therefore, the value of $\chi_q$ calculated from Eqs. (1), and (3) is reasonably accurate. Also, preferential diffusion (neglected in obtaining $\xi_{st}$ and $T_{st}$) surprisingly does not appear to influence the scalar dissipation rate at extinction.

The scalar dissipation rate at extinction $\chi_q$, obtained using activation-energy asymptotic analysis employing one-step chemistry, is [36, 37, 44]

$$\chi_q = \frac{2Y_{F,1}A_o\rho_{st}{T_{st}}^6 R^3 {\xi_{st}}^2(1-\xi_{st})^2}{W_F {E_o}^3 (T_{st}-T_u)^3} \exp\left(-1-\frac{E_o}{RT_{st}}\right). \tag{4}$$

The product $\rho_{st}T_{st}$ is presumed to be constant. From Eq. (4) it follows that a plot of $\ln\left\{\chi_q(T_{st}-T_u)^3/[Y_{F,1}{T_{st}}^5{\xi_{st}}^2(1-\xi_{st})^2]\right\}$ as a function of $1/T_{st}$ represents an Arrhenius diagram. The slope of this plot gives $E_o$. The experimental and numerical values of $a_q$ shown in Figs. 3 and 4 are used to calculate $\chi_q$ at extinction using Eq. (3). Using Equation (4), Arrhenius diagrams are constructed. Using the results in Fig. 3, the values of $E_o$ obtained using experimental data, Mechanism A, and Mechanism B are 82 kJ/mol, 182 kJ/mol, and 69 kJ/mol respectively. Using the results in Fig. 4, the values of $E_o$ obtained using experimental data, Mechanism A, and Mechanism B are 109 kJ/mol, 195 kJ/mol, and 79 kJ/mol respectively. Therefore, qualitative agreement of Mechanism B with experiments is better than that between Mechanism A and the experiments.

Figure 5 shows calculated concentration profiles of $H_2$, $O_2$, $H_2O$, $CF_3Br$, HBr, H, and Br, and the temperature profile. The profiles are calculated with 16 % $H_2$ by volume in the fuel stream, 2.5 % $CF_3Br$ by volume in the oxidizing stream, and for $a = 150\,s^{-1}$. Figure 5 shows HBr and Br to reach their peak values near the region where $CF_3Br$ vanishes. This region will be referred to as the $CF_3Br$-consumption layer. This layer was also present in hydrocarbon flames inhibited with $CF_3Br$ [5, 9]. In hydrocarbon flames, there was a region called the fuel-consumption layer where the fuel was consumed [5, 9]. The region between the fuel-consumption layer and the $CF_3Br$-consumption layer was called the oxidation layer [5, 9]. In the oxidation layer, oxygen is consumed, and the temperature and H-radicals were found to reach their peak values [5, 9]. The structure of hydrogen flames appears to be different from that of hydrocarbon flames. Figure 5 shows both hydrogen and oxygen to be consumed together in the region to the left of the $CF_3Br$-consumption layer. The concentrations of H, and $H_2O$ and temperature reach their peak values in the region to the left of the $CF_3Br$-consumption layer. Therefore, there are significant differences between the structure of inhibited hydrogen flames and hydrocarbon flames.

## Concluding Remarks

An experimental and numerical study is conducted to characterize the influence of $CF_3Br$ on the structure and critical conditions of extinction of hydrogen flames. The rate of the key elementary reaction $CF_3Br + H = CF_3 + HBr$, which contributes to the consumption of $CF_3Br$, is measured. Numerical calculations are performed using two detailed chemical-kinetic mechanisms. The critical conditions of extinction calculated using Mechanism B are found to agree well with the measurements. Numerical calculations were also performed employing Mechanism A using the rate data for the elementary reaction $CF_3Br + H = CF_3 + HBr$ shown in Table II of Ref. [11]. The critical conditions of extinction calculated using this rate for $CF_3Br + H = CF_3 + HBr$ were nearly identical to those calculated with the improved rate for this reaction. Mechanism A and Mechanism B include similar sets of reactions for describing the chemistry of HBr and Br, but with a few significant deviations. These are discussed by evaluating the values of the rate constants at 1200 K, a representative temperature for the flames studied here. The rate constant for Br atom recombination employed in Mechanism B is approximately twenty-six times smaller than that employed in Mechanism A, and therefore leads to a reduced role for $Br_2$ in Mechanism B. This is partly compensated by the fact that the rate constant for the reaction $H + Br_2 = HBr + Br$ in Mechanism B is larger by a factor of 1.6. In Mechanism A the rate constant for the H + Br recombination to form HBr and the rate constants for HBr reactions with OH and O are significantly larger than those in Mechanism B, by factors of 1.8, 15 and 91, respectively, although the rate constants employed

for the major flame radical removal pathway H + HBr are similar. There are also notable differences in the treatment of the chemistry of decomposition of $CF_3Br$. The rate constant for unimolecular decomposition of $CF_3Br$ at 1200 K in Mechanism A is half that in Mechanism B, whereas the rate constant for reaction of $CF_3Br$ with H atoms is larger by a factor of 1.5. The revised rate constant employed here is larger still, by an additional factor of two.

## Acknowledgments

The numerical calculations were performed using the "FLAMEMASTER," which is a computer program developed at RWTH Aachen by H. Pitsch, M. Bollig, J. Göttgens and P. Terhoeven. The authors thank Professor F. A. Williams for helpful discussions. The work at The University of California at San Diego was supported by the U. S. Army Research Office through Grant # ARO DAAH-95-1-0108. The work at the University of North Texas at was supported by the Robert A. Welch Foundation (Grant B-1174), the Air Force Office of Scientific Research, and the UNT Faculty Research Fund.

## References


[1] W. M. Pitts, M. R. Nyden, R. G. Gann, W. G. Mallard, and W. Tsang. In *Construction of an Exploratory List of Chemicals to Initiate the Search for Halon Alternatives*, volume 1279 of *NIST Technical Note*, pages 14–40, Washington, D. C., August 1990. U. S. Department of Commerce, National Institute of Standards and Technology.

[2] E. C. Creitz. *Journal of Research of the National Bureau of Standards*, 65 A:389–396, 1961.

[3] R. F. Kubin, R. H. Knipe, and A. S. Gordon. In R. G. Gann, editor, *Halogenated Fire Suppressants*, volume 16, pages 183–207, Washington, D. C., 1975. American Chemical Society.

[4] A. R. Masri. *Combustion Science and Technology*, 96:189–212, 1994.

[5] A. Hamins, D. Trees, K. Seshadri, and H. K. Chelliah. *Combustion and Flame*, 99:221–230, 1994.

[6] D. Trees, K. Seshadri, and A. Hamins. In A. W. Miziolek and W. Tsang, editors, *Halon Replacements: Technology and Science*, volume 611 of *ACS Symposium Series*, chapter 17, pages 190–203. American Chemical Society, Washington, D. C., 1995.

[7] K. Seshadri and N. Ilincic. *Combustion and Flame*, 101(3):271–286, May 1995.

[8] D. Trees. *Chemical Inhibition of Diffusion Flames.* PhD thesis, Institut für Allgemeine Mechanik, RWTH Aachen, Germany, Shaker Verlag, Aachen, 1996. ISBN 3-8265-1922-1.

[9] D. Trees, A. Grudno, and K. Seshadri. *Combustion Science and Technology*, 124(1-6):311, 1997.

[10] A. Grudno and K. Seshadri. *Combustion and Flame*, 112:418–437, 1998.

[11] C. K. Westbrook. *Combustion Science and Technology*, 34:201–225, 1983.

[12] A. A. Westenberg and N. J. DeHass. *J. Chem. Phys.*, 67:2388, 1977.

[13] G. Le Bras and J. Combourieu. *J. Int. Chem. Kinet.*, 10:1205, 1978.

[14] D. M. Silver and N. DeHaas. *J. Chem. Phys.*, 74:1745, 1981.

[15] J. C. Biordi, C. P. Lazzara, and J. F. Papp. *Combustion and Flame*, 26:57, 1976.

[16] L. D. Petrova, V. V. Azatyan, A. N. Baratov, V. I. Makeev, and E. E. Kondenko. *Bull. Acad. Sci. USSR, Div. Chem. Sci.*, 25:879, 1976. Russian Original page 90.

[17] J. C. Biordi, C. P. Lazzara, and J. F. Papp. *J. Phys. Chem*, 81:1139, 1977.

[18] D. L. Baulch, J. Duxbury, S. J. Grant, and D. C. Montague. *J. Phys. Chem. Ref. Data.*, 10, 1981. Suppl. 1.

[19] Y. Hidaka, T. Nakamura, H. Kawano, and T. Koike. *Int. J. Chem. Kinet.*, 25:983, 1993.

[20] K. Seshadri and F. A. Williams. *International Journal of Heat and Mass Transfer*, 21(2):251–253, 1978.

[21] Y. Shi and P. J. Marshall. *J. Phys. Chem*, 95:1654, 1991.

[22] L. Ding and P. J. Marshall. *J. Phys. Chem.*, 96:2197, 1992.

[23] A. Goumri, W.-J Yuan, L. Ding, Y. Shi, and P. J. Marshall. *P. Chem. Phys.*, 177:233, 1993.

[24] L. A. Curtiss, K. Raghavachari, G. W. Trucks, and J. A. Pople. *J. Chem. Phys.*, 94:7221, 1991.

[25] M. N. Glukhovtsev, A. Pross, M. P. McGarth, and L.. Radom. *J. Chem. Phys.*, 103:1878, 1995.

[26] R. J. Berry and P. Marshall. *Int. J. Chem. Kinetics*, 1998. in press.

[27] J. I. Steinfeld, J. S. Franscisco, and W. L. Hasse. *Chemical Kinetics and Dynamics*, chapter 10. Prentice Hall, Englewood Cliffs, 1989.

[28] H. S. Johnston. *Gas Phase Reaction Rate Theory*, chapter 2. Ronald, New York, 1966.

[29] M. W. Chase, C. A. Davies, J. R. Downey, D. J. Frurip, R. A. McDonald, and A. N. Syverud. In *JANNAF Thermochemical Tables*, volume 14 of *J. Phys. Chem. Ref. Data, Suppl. No. 1.* 3rd edition, 1985.

[30] M. D. Smooke, I. K. Puri, and K. Seshadri. In *Twenty-first Symposium (International) on Combustion*, pages 1783–1792, Pittsburgh, Pennsylvania, 1986. The Combustion Institute.

[31] N. Peters. In N. Peters and B. Rogg, editors, *Reduced Kinetic Mechanisms for Applications in Combustion Systems*, volume m15 of *Lecture Notes in Physics*, chapter 1, pages 1–13. Springer-Verlag, Heidelberg, 1993.

[32] H. Pitsch. Entwicklung eines Programmpaketes zur Berechnung eindimensionaler Flammen am Beispiel einer Gegenstromdiffusionsflamme. Master's thesis, RWTH Aachen, Germany, 1993.

[33] Inhibition Mechanism obtained from http://www.nist.gov/cstl/div836/ckmech/Mechanisms.html, 1996.

[34] V. Babushok, T. Noto, D. R. F. Burgess, A. Hamins, and W. Tsang. *Combustion and Flame*, 107(4):351–367, 1996.

[35] T. Noto, V. Babushok, A. Hamins, and W. Tsang. *Combustion and Flame*, 112:147–160, 1998.

[36] N. Peters. Local quenching due to flame stretch and non-premixed turbulent combustion. *Combustion Science and Technology*, 30:1–17, 1983.

[37] N. Peters. *Progress in Energy and Combustion Science*, 10:319–339, 1984.

[38] F. A. Williams. *Combustion Theory.* Addison-Wesley Publishing Company, Redwood City, CA, 2 edition, 1985.

[39] A. Liñán and F. A. Williams. *Fundamental Aspects of Combustion*, volume 34 of *Oxford Engineering Science Series.* Oxford University Press, New York, 1993.

[40] K. Seshadri and F. A. Williams. In P. A. Libby and F. A. Williams, editors, *Turbulent Reacting Flows*, pages 153–210. Academic Press, San Diego, California, 1994.

[41] K. Seshadri. In *Twenty-Sixth Symposium (International) on Combustion,*, pages 831–846, Pittsburgh, Pennsylvania, 1996. The Combustion Institute.

[42] A. Grudno and K. Seshadri. *Combustion Science and Technology,*, 112:201, 1996.

[43] J. S. Kim and F. A. Williams. *SIAM Journal on Applied Mathematics*, 53:1551–1566, 1993.

[44] B. Yang and K. Seshadri. *Combustion Science and Technology*, 88:115–132, 1992.

# List of Figures

Figure 1: Comparison of measured and computed rate constants for H + $CF_3Br \rightarrow CF_3$ + HBr with literature values. Circles: FP-RF measurements, $k_m$; open—$NH_3$ used as H-atom source; filled—$H_2O$ used as H-atom source, $k_c$ (present work). Dashed line: transition state theory result (present work). Triangle: measurement by Westenberg et al. (Ref. [12]). Square: measurement by Le Bras et al. (Ref. [13]). Solid lines: fits to literature values: 1 Silver et al. (Ref. [14]); 2 Hidaka et al. (Ref. [19]); 3 Biordi et al. (Ref. ( [17]); 4 Baulch et al. (Ref. [18]); 5 Petrova et al. (Ref. [16]); 6 Biordi et al. (Ref. [15]).

Figure 2: Plot of pseudo-first-order decay constant for loss of H-atoms in the presence of excess $CF_3Br$ at 860 K and 140 mbar total pressure. The inset shows the measured intensity $I_f$ as a function of time $t$. The filled point is derived from the decay of fluorescence plus background from scattered light shown in the inset.

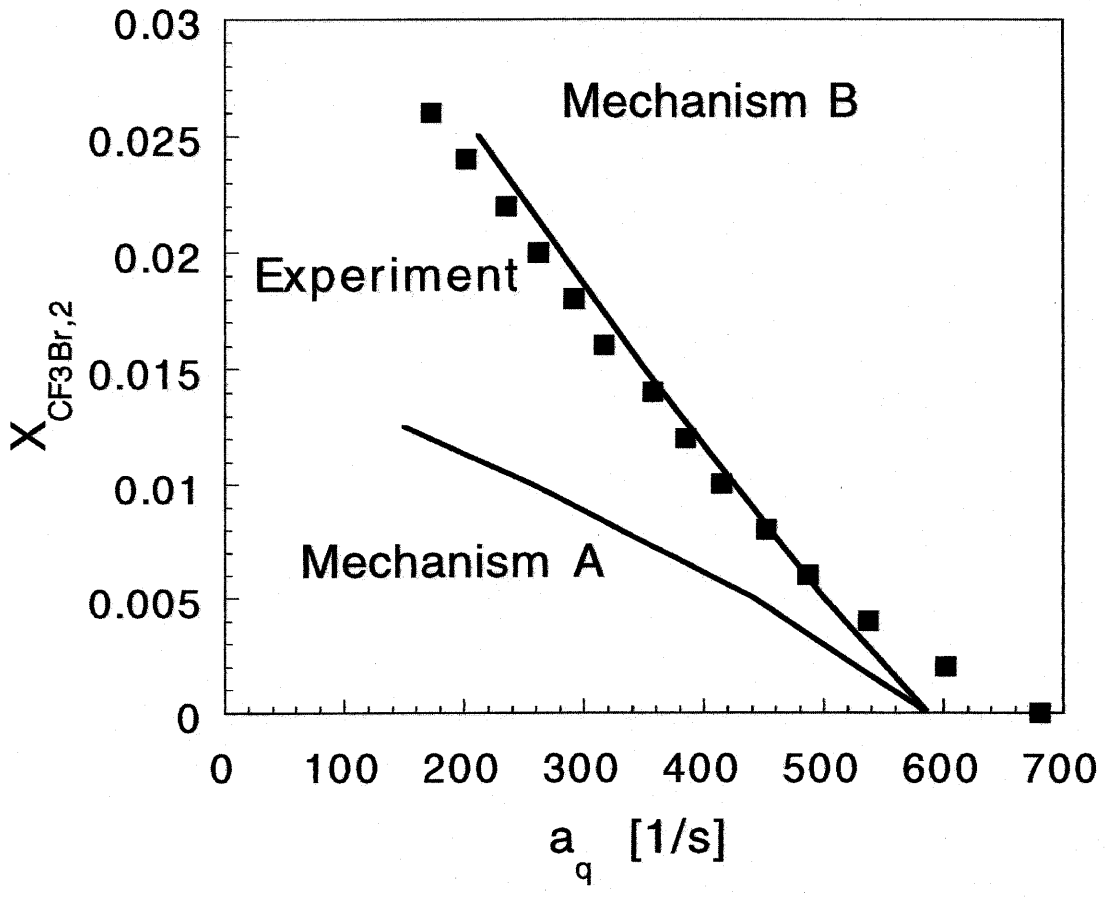


Figure 3: The mole fraction of $CF_3Br$ in the oxidizing stream $X_{CF_3Br,2}$ as a function of the strain rate $a_q$ at extinction. The fuel stream is comprised 16% $H_2$ and 84% $N_2$ by volume. The symbols represent experimental data. The experimental data is compared with results of numerical calculations performed using Mechanism A and Mechanism B.

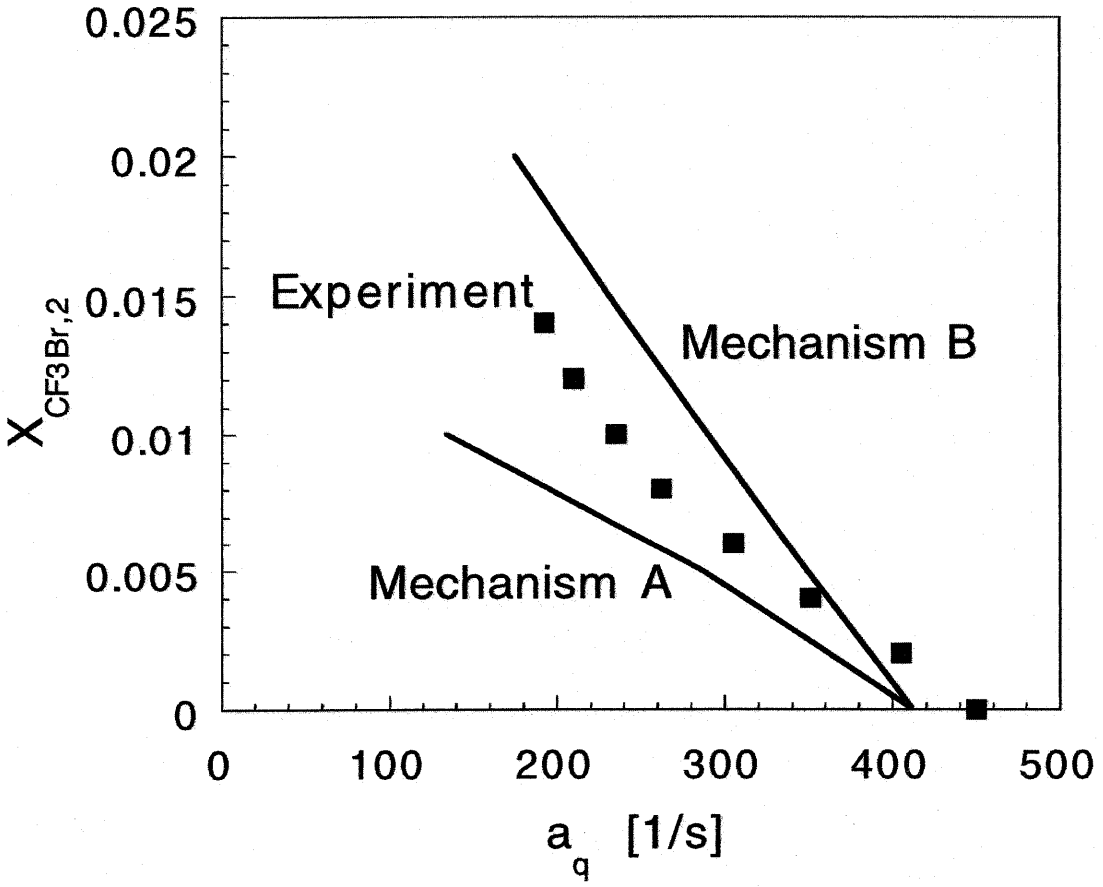


Figure 4: The mole fraction of $CF_3Br$ in the oxidizing stream $X_{CF_3Br,2}$ as a function of the strain rate $a_q$ at extinction. The fuel stream is comprised 15% $H_2$ and 85% $N_2$ by volume. The symbols represent experimental data. The experimental data is compared with results of numerical calculations performed using Mechanism A and Mechanism B.

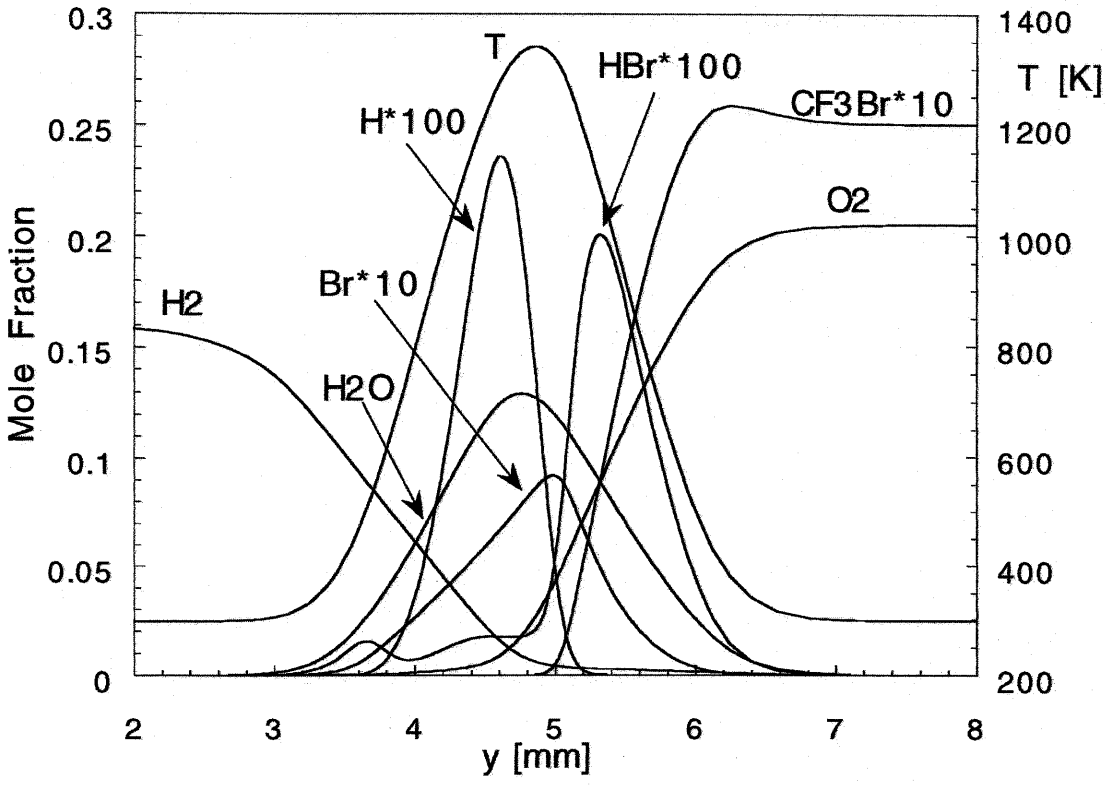


Figure 5: Concentration profiles of $H_2$, $O_2$, $H_2O$, $CF_3Br$, HBr, H, and Br, and the temperature profile calculated using Mechanism B for $a = 150$. The fuel stream is made up of 16% $H_2$ and 84% $N_2$ by volume. The oxidizing stream contains 2.5 % $CF_3Br$ by volume.

## References


[1] W. M. Pitts, M. R. Nyden, R. G. Gann, W. G. Mallard, and W. Tsang. Current understanding. In *Construction of an Exploratory List of Chemicals to Initiate the Search for Halon Alternatives*, volume 1279 of *NIST Technical Note*, pages 14–40, Washington, D. C., August 1990. U. S. Department of Commerce, National Institute of Standards and Technology.

[2] E. C. Creitz. Inhibition of diffusion flames by methyl bromide and trifluromethyl bromide applied to the fuel and oxygen sides of the reaction zone. *Journal of Research of the National Bureau of Standards*, 65 A:389–396, 1961.

[3] R. F. Kubin, R. H. Knipe, and A. S. Gordon. Halomethane and nitrogen quenching of hydrogen and hydrocarbon diffusion and premixed flames. In R. G. Gann, editor, *Halogenated Fire Suppressants*, volume 16, pages 183–207, Washington, D. C., 1975. American Chemical Society.

[4] A. R. Masri. Chemical inhibition of nonpremixed flames of hydrocarbon fuels with $CF_3Br$. *Combustion Science and Technology*, 96:189–212, 1994.

[5] A. Hamins, D. Trees, K. Seshadri, and H. K. Chelliah. Extinction of nonpremixed flames with halogenated fire suppressants. *Combustion and Flame*, 99:221–230, 1994.

[6] D. Trees, K. Seshadri, and A. Hamins. Experimental studies of diffusion flame extinction with halogenated and inert fire suppressants. In A. W. Miziolek and W. Tsang, editors, *Halon Replacements: Technology and Science*, volume 611 of *ACS Symposium Series*, chapter 17, pages 190–203. American Chemical Society, Washington, D. C., 1995.

[7] K. Seshadri and N. Ilincic. The asymptotic structure of inhibited nonpremixed methane-air flames. *Combustion and Flame*, 101(3):271–286, May 1995.

[8] D. Trees. *Chemical Inhibition of Diffusion Flames.* PhD thesis, Institut für Allgemeine Mechanik, RWTH Aachen, Germany, Shaker Verlag, Aachen, 1996. ISBN 3-8265-1922-1.

[9] D. Trees, A. Grudno, and K. Seshadri. Experimental and numerical studies on chemical inhibition of nonpremixed methane flames by $CF_3Br$. *Combustion Science and Technology*, 124(1-6):311, 1997.

[10] A. Grudno and K. Seshadri. Rate-ratio asymptotic analysis of inhibition of nonpremixed methane-air flames by $CF_3Br$. *Combustion and Flame*, 112:418–437, 1998.

[11] C. K. Westbrook. Numerical modeling of flame inhibition by $CF_3Br$. *Combustion Science and Technology*, 34:201–225, 1983.

[12] A. A. Westenberg and N. J. DeHass. *J. Chem. Phys.*, 67:2388, 1977.

[13] G. Le Bras and J. Combourieu. *J. Int. Chem. Kinet.*, 10:1205, 1978.

[14] D. M. Silver and N. DeHaas. *J. Chem. Phys.*, 74:1745, 1981.

[15] J. C. Biordi, C. P. Lazzara, and J. F. Papp. *Combustion and Flame*, 26:57, 1976.

[16] L. D. Petrova, V. V. Azatyan, A. N. Baratov, V. I. Makeev, and E. E. Kondenko. *Bull. Acad. Sci. USSR, Div. Chem. Sci.*, 25:879, 1976. Russian Original page 90.

[17] J. C. Biordi, C. P. Lazzara, and J. F. Papp. *J. Phys. Chem*, 81:1139, 1977.

[18] D. L. Baulch, J. Duxbury, S. J. Grant, and D. C. Montague. *J. Phys. Chem. Ref. Data.*, 10, 1981. Suppl. 1.

[19] Y. Hidaka, T. Nakamura, H. Kawano, and T. Koike. *Int. J. Chem. Kinet.*, 25:983, 1993.

[20] K. Seshadri and F. A. Williams. Laminar flow between parallel plates with injection of a reactant at high Reynolds number. *International Journal of Heat and Mass Transfer*, 21(2):251–253, 1978.

[21] Y. Shi and P. J. Marshall. *J. Phys. Chem*, 95:1654, 1991.

[22] L. Ding and P. J. Marshall. *J. Phys. Chem.*, 96:2197, 1992.

[23] A. Goumri, W.-J Yuan, L. Ding, Y. Shi, and P. J. Marshall. *P. Chem. Phys.*, 177:233, 1993.

[24] L. A. Curtiss, K. Raghavachari, G. W. Trucks, and J. A. Pople. *J. Chem. Phys.*, 94:7221, 1991.

[25] M. N. Glukhovtsev, A. Pross, M. P. McGarth, and L.. Radom. *J. Chem. Phys.*, 103:1878, 1995.

[26] R. J. Berry and P. Marshall. *Int. J. Chem. Kinetics*, 1998. in press.

[27] J. I. Steinfeld, J. S. Franscisco, and W. L. Hasse. *Chemical Kinetics and Dynamics*, chapter 10. Prentice Hall, Englewood Cliffs, 1989.

[28] H. S. Johnston. *Gas Phase Reaction Rate Theory*, chapter 2. Ronald, New York, 1966.

[29] M. W. Chase, C. A. Davies, J. R. Downey, D. J. Frurip, R. A. McDonald, and A. N. Syverud. In *JANNAF Thermochemical Tables*, volume 14 of *J. Phys. Chem. Ref. Data, Suppl. No. 1.* 3rd edition, 1985.

[30] M. D. Smooke, I. K. Puri, and K. Seshadri. A comparison between numerical calculations and experimental measurements of the structure of a counterflow diffusion flame burning diluted methane in diluted air. In *Twenty-first Symposium (International) on Combustion*, pages 1783–1792, Pittsburgh, Pennsylvania, 1986. The Combustion Institute.

[31] N. Peters. Flame calculations with reduced mechanisms - an outline. In N. Peters and B. Rogg, editors, *Reduced Kinetic Mechanisms for Applications in Combustion Systems*, volume m15 of *Lecture Notes in Physics*, chapter 1, pages 1–13. Springer-Verlag, Heidelberg, 1993.

[32] H. Pitsch. Entwicklung eines Programmpaketes zur Berechnung eindimensionaler Flammen am Beispiel einer Gegenstromdiffusionsflamme. Master's thesis, RWTH Aachen, Germany, 1993.

[33] Inhibition Mechanism obtained from http://www.nist.gov/cstl/div836/ckmech/Mechanisms.html, 1996.

[34] V. Babushok, T. Noto, D. R. F. Burgess, A. Hamins, and W. Tsang. Influence of $CF_3I$, $CF_3Br$, and $CF_3H$ on the high-temperature combustion of methane. *Combustion and Flame*, 107(4):351–367, 1996.

[35] T. Noto, V. Babushok, A. Hamins, and W. Tsang. Inhibition effectiveness of halogenated compounds. *Combustion and Flame*, 112:147–160, 1998.

[36] N. Peters. Local quenching due to flame stretch and non-premixed turbulent combustion. *Combustion Science and Technology*, 30:1–17, 1983.

[37] N. Peters. Laminar diffusion flamelet models in non-premixed turbulent combustion. *Progress in Energy and Combustion Science*, 10:319–339, 1984.

[38] F. A. Williams. *Combustion Theory*. Addison-Wesley Publishing Company, Redwood City, CA, 2 edition, 1985.

[39] A. Liñán and F. A. Williams. *Fundamental Aspects of Combustion*, volume 34 of *Oxford Engineering Science Series*. Oxford University Press, New York, 1993.

[40] K. Seshadri and F. A. Williams. Reduced chemical systems and their application in turbulent combustion. In P. A. Libby and F. A. Williams, editors, *Turbulent Reacting Flows*, pages 153–210. Academic Press, San Diego, California, 1994.

[41] K. Seshadri. Multistep asymptotic analyses of flame structures. In *Twenty-Sixth Symposium (International) on Combustion,*, pages 831–846, Pittsburgh, Pennsylvania, 1996. The Combustion Institute.

[42] A. Grudno and K. Seshadri. Characteristic residence times of laminar nonpremixed flames at extinction. *Combustion Science and Technology,*, 112:201, 1996.

[43] J. S. Kim and F. A. Williams. Structures of flow and mixture-fraction fields for counterflow diffusion flames with small stoichiometric mixture fractions. *SIAM Journal on Applied Mathematics*, 53:1551–1566, 1993.

[44] B. Yang and K. Seshadri. Asymptotic analysis of the structure of nonpremixed methane air flames using reduced chemistry. *Combustion Science and Technology*, 88:115–132, 1992.